Postzygotic isolation drives genomic speciation between highly cryptic Hypocnemis antbirds from Amazonia

Cronemberger, Aurea A.

2020-11

Cronemberger , A A , Aleixo , A , Mikkelsen , E K & Weir , J T 2020 , ' Postzygotic isolation drives genomic speciation between highly cryptic Hypocnemis antbirds from Amazonia ' , Evolution , vol. 74 , no. 11 , pp. 2512-2525 . https://doi.org/10.1111/evo.14103

http://hdl.handle.net/10138/335106
https://doi.org/10.1111/evo.14103

acceptedVersion

doi:10.1111/evo.14

Postzygotic isolation drives genomic speciation between highly cryptic *Hypocnemis* antbirds from Amazonia

Áurea A. Cronemberger,[1,2,3] Alexandre Aleixo,[3,4] Else K. Mikkelsen,[1,2] and Jason T. Weir[1,2,5,6]

[1]*Department of Ecology and Evolutionary Biology, University of Toronto, Toronto, Canada*

[2]*Department of Biological Sciences, University of Toronto Scarborough, Toronto, Canada*

[3]*Pós-graduação em Biodiversidade e Evolução, Museu Paraense Emílio Goeldi, Belém, Brazil*

[4]*Finnish Museum of Natural History, University of Helsinki, Helsinki, Finland*

[5]*Department of Natural History, Royal Ontario Museum, Toronto, Canada*

[6]*E-mail: jason.weir@utoronto.ca*

Received February 19, 2020

Accepted August 28, 2020

How species evolve reproductive isolation in the species-rich Amazon basin is poorly understood in vertebrates. Here, we sequenced a reference genome and used a genome-wide sample of SNPs to analyze a hybrid zone between two highly cryptic species of *Hypocnemis* warbling-antbirds—the Rondonia warbling-antbird (*H. ochrogyna*) and Spix's warbling-antbird (*H. striata*)—in a headwater region of southern Amazonia. We found that both species commonly hybridize, producing F_1s and a variety of backcrosses with each species but we detected only one F_2-like hybrid. Patterns of heterozygosity, hybrid index, and interchromosomal linkage disequilibrium in hybrid populations closely match expectations under strong postzygotic isolation. Hybrid zone width (15.4 km) was much narrower than expected (211 km) indicating strong selection against hybrids. A remarkably high degree of concordance in cline centers and widths across loci, and a lack of reduced interspecific F_{st} between populations close to versus far from the contact zone, suggest that genetic incompatibilities have rendered most of the genome immune to introgression. These results support intrinsic postzygotic isolation as a driver of speciation in a moderately young cryptic species pair from the Amazon and suggest that species richness of the Amazon may be grossly underestimated.

KEY WORDS: Amazon, genetic incompatibility, hybridization, *Hypocnemis*, postzygotic reproductive isolation, speciation.

Species richness of birds and other groups is exceptionally high in Amazonia, and many phylogeographic assessments of widespread Amazonian taxa find that currently defined species comprise complexes of taxa which are deeply diverged genetically despite limited morphological and behavioral divergence (e.g. Silva et al. 2019). Some of these taxa are so similar morphologically that they have not previously been recognized taxonomically, even at the subspecies level (e.g. phylogroups within the Spot-backed Antbird; Fernandes et al. 2014). Whether such cryptic taxa are reproductively isolated and deserve species status, leading to even higher levels of Amazonian species richness, or simply represent geographically differentiated populations of polytypic species is difficult to infer, but could have profound consequences on our understanding of species richness in what is already recognized as the most species-rich region of the planet.

Recent attempts to address speciation in morphologically cryptic taxa of Amazonian birds have largely focused on behavior, with detailed analyses of vocalizations often showing minor, but diagnosable differences which have often been used to reassess species boundaries under the assumption that consistent variations in song or calls between allopatric populations have rendered them reproductively isolated (e.g. *Hypocnemis*, Isler et al. 2007a; *Willisornis*, Isler and Whitney 2011; *Percnostola*, Isler et al. 2007b). In some cases, additional clear evidence

for speciation for specific taxa has been uncovered (e.g. broad sympatry rather than allopatry was demonstrated for *Hypocnemis subflava* and *H. peruviana* and these appear to mate assortatively in sympatry; Isler et al. 2007a), but for many taxa no additional evidence is available. However, recent comparative analyses involving playback experiments on male birds found that Amazonian species continue to respond to playback of the songs of closely related taxa for much longer on average than at high latitudes, suggesting that the slight variations in song that differentiate many cryptic, allopatric pairs of Amazonian taxa may not be serving as strong discriminatory cues, at least for male birds (Weir and Price 2019). Whether weak species discrimination will be true of females also is much harder to test in the field. A slow rate of song divergence near the equator (Weir and Wheatcroft 2011; Weir et al. 2012) coupled with a slow rate of male song discrimination (Weir and Price 2019) might argue against song-based premating isolation as a key driver of speciation in Amazonian birds (see also Pulido-Santacruz et al. 2018).

Parapatric contact zones provide a useful tool for assessing levels of reproductive isolation between cryptic Amazonian taxa. A lack of frequent hybridization along contact zones would provide evidence that cryptic taxa have acquired strong premating isolation and are behaving as distinct species. Genome-wide datasets were recently used to document local syntopy between seven pairs of species and subspecies which are largely allopatric, but which form narrow contact zones in the headwater region between the Teles Pires and Xingu rivers of southern Amazonia (Weir et al. 2015). Four of the seven pairs of taxa were highly cryptic and required multilocus analyses to detect local syntopy. Hybrids were discovered in all seven species pairs, while those pairs sampled in detail in regions of syntopy revealed that hybridization was frequent, even between taxa as old as four million years (Pulido-Santacruz et al. 2018).

The presence of old hybrid zones in the Amazon demonstrates that premating isolating barriers are often poorly developed, even after several million years of divergence. However, the dynamics of hybridization along parapatric contact zones can also provide important insight into levels of intrinsic postzygotic isolation. A recent genome-wide assessment of hybrid zones in two pairs of cryptic Amazonian bird species revealed evidence that speciation was essentially complete and was driven primarily by the accumulation of intrinsic postzygotic isolation. First, while plenty of F_1 hybrids and backcrosses of these into parental populations were documented, entire classes of early generation hybrids representing the most heavily recombined genotypes between the parental species were rare or missing from hybrid zones. Simulations with high levels of assortative mating (based on genomic similarity) were incapable of producing an absence of these hybrid classes (due to a lack of selection against F_2 and other early generation backcrosses), but simulations with postzygotic isolation (i.e. in the form of genetic incompatibilities) produced nearly identical results (F_2 hybrids and other early generation hybrid classes with heavily recombined genomes were selected against). Second, these hybrid zones also revealed remarkably little variation in geographic and genomic cline centers or widths across individual loci. Substantial variability in hybrid zone dynamics is expected under neutral dynamics and is often observed in natural hybrid zones (e.g. Payseur 2010). Its absence suggests that most of the genome is behaving in a concerted fashion. The accumulation of many genetic incompatibilities across the genome causes neutral regions that should otherwise be free to introgress to be closely linked to loci that are selected against in the wrong genetic background. These results support the role of intrinsic postzygotic isolation in driving speciation in cryptic Amazonian taxa, but the taxon-pairs studied were old (2.5 to 4 million years), and postzygotic isolation, which is expected to accumulate as a function of genome differentiation (Orr 1995; Orr and Turelli 2001), might be expected to have accumulated to high levels in such old taxa pairs. It remains to be determined if postzygotic isolation is also capable of driving speciation on shorter time scales of 1 to 2 million years—a time frame over which a great many cryptic pairs of Amazonian taxa (e.g. subspecies and closely related congeneric species) have been diverging (Silva et al. 2019).

The *Hypocnemis cantator* complex possesses cryptic taxa that span a range of divergence dates and this provides an excellent opportunity to study the process of Amazonian speciation that involves minimal morphological or behavioural divergence. Six currently recognized species in this complex (*H. cantator, H. flavescens, H. peruviana, H. rondoni, H. ochrogyna*, and *H. striata*) are fully allopatric or parapatric (we exclude the sister group to this complex, *H. subflava*, which, though generally included, differs substantially in plumage and is now known to be sympatric with *H. peruviana* over a major portion of its lowland geographic distribution), and are highly similar in plumage (with some essentially undiagnosable even in the hand; see Whitney et al. 2013). Though they differ consistently in songs and/or calls—the key reason they were recently split into distinct species (Isler et al. 2007a; del Hoyo and Collar 2016)—vocal differences do not seem strongly pronounced (e.g. Fig. 1), and recent playback experiments between several taxon pairs in this complex (songs of various taxa were played to territorial males or male/female pairs of *H. peruviana* and response to heterotypic versus contypic song was recorded) generally suggested weak song discrimination (Weir and Price 2019). Two members of this complex, *H. ochrogyna* and *H. striata striata* (Fig. 1), form a parapatric contact zone in the headwaters between the Teles Pires and Xingu Rivers (Figs. 2, 3) where both species and a single hybrid between them were recently discovered in syntopy (Weir et al. 2015). This species pair is closely related

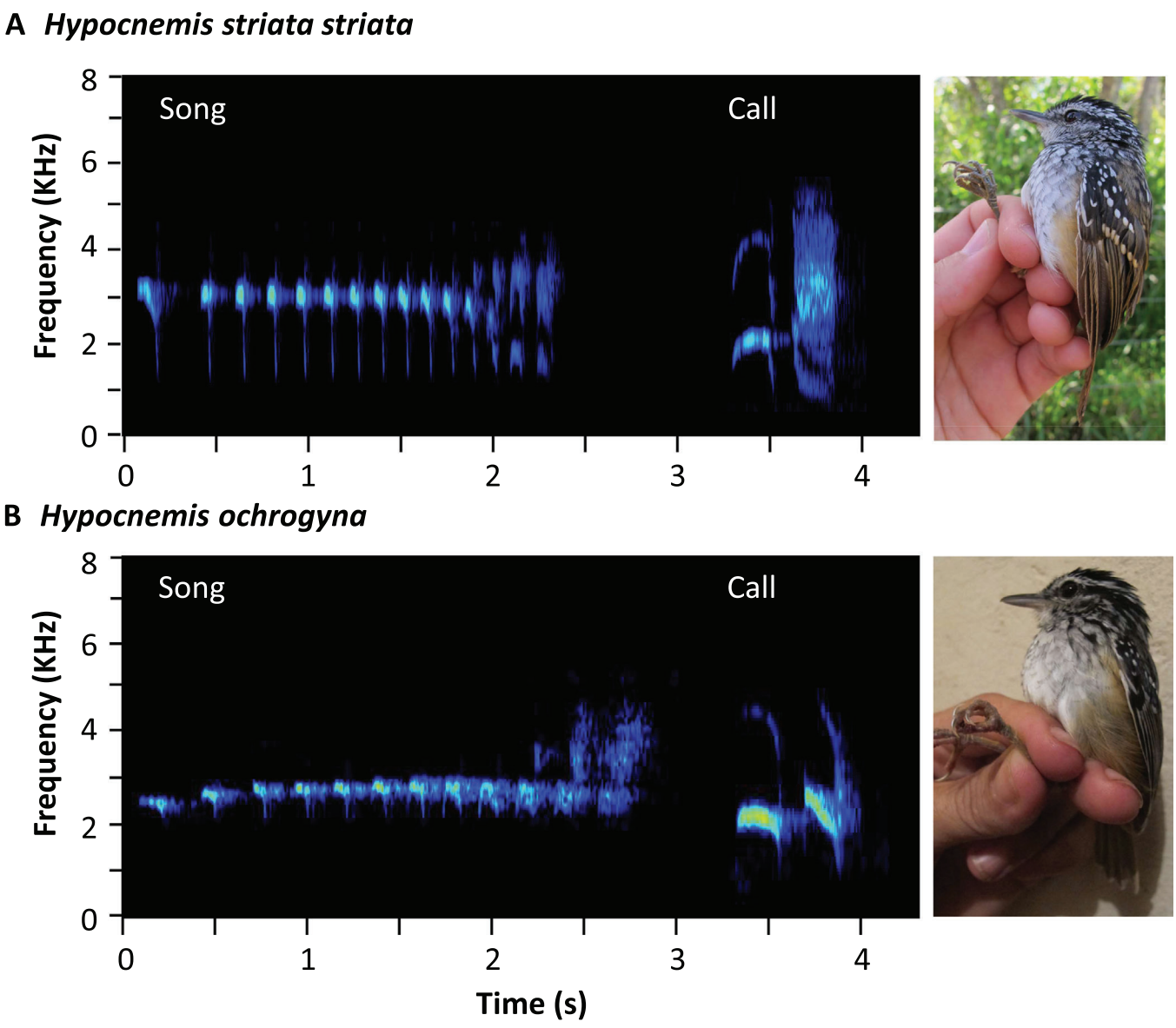

Figure 1. Examples of sonograms of male song and call and photos of (A) *Hypocnemis striata striata* (photo: specimen PPS 146, 9.940°S, 54.342°W; song from www.xeno-canto.org: XC89567, -9.598°S, 55.931°W; call from our recording: 10.513°S, 54.409°W) and (B) *H. ochrogyna* (photo: specimen MSF 167, 13.126°S, 54.429°W; song from our recording: 12.531°S, 54.348°W; call from xeno-canto: XC171010: 13.817°S, 59.661°W). Sonograms have been edited to exclude background vocalizations of other birds.

with mitochondrial markers placing *H. ochrogyna* as sister to the recently recognized *H. rondoni*, and these together are sister to *H. striata* (Whitney et al. 2013), while hundreds of nuclear markers indicate *H. striata* and *H. rondoni* are sisters with *H. ochrogyna* sister to these (Cronemberger, unpubl. data). While songs differ primarily in pace (Fig. 1; Isler et al. 2007a), this species pair are nearly identical in plumage with *H. striata* reported to have slightly more black on the back on average than *H. ochrogyna* (del Hoyo and Collar 2016), though differences are not diagnostic in our experience. Mitochondrial dating suggests they diverged from a common ancestor somewhat less than two million years ago (Weir et al. 2015; Silva et al. 2019), and thus, provide an ideal opportunity to study whether intrinsic postzygotic isolation is capable of promoting speciation in a highly cryptic taxon pair of younger age.

To address the role of intrinsic postzygotic isolation in driving speciation in *H. ochrogyna* and *H. striata*, we assembled a de novo draft genome of *H. ochrogyna*, and obtained a large dataset of more than 93,000 SNPs spread across the genome from a large series of individuals obtained from transects bisecting two contact zone populations. We analyzed hybrid index, observed heterozygosity and linkage disequilibrium to assess whether selection has operated against F_2 and similar hybrid classes with highly recombined genomes. We performed geographic cline

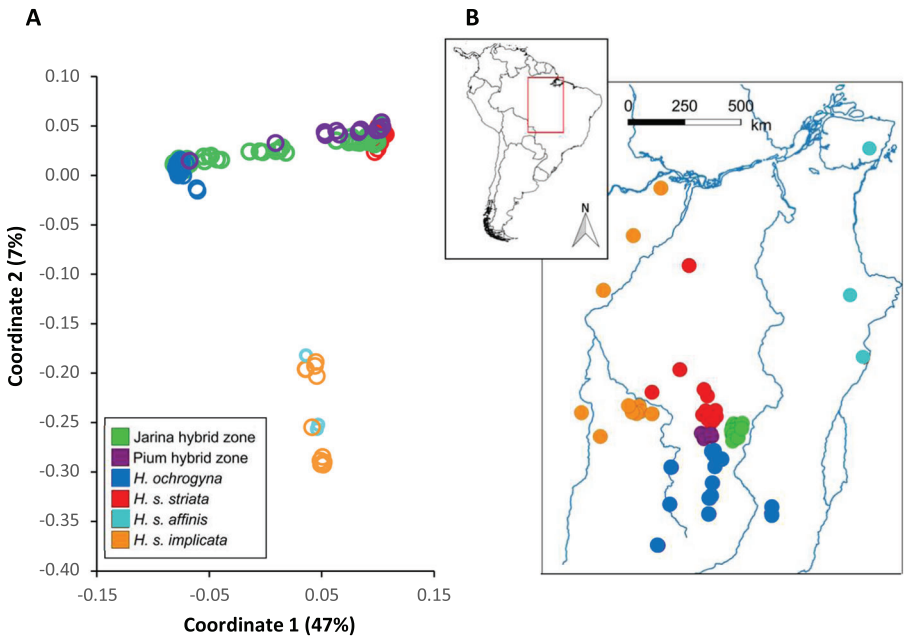

Figure 2. **Sampling localities and principal coordinate analyses of 20,440 SNPs for *Hypocnemis striata* and *H. ochrogyna* and their hybrids. (A) Principal coordinate analysis including all *H. ochrogyna* and *H. striata* specimens sampled with the proportion of variance explained shown for plotted axes. (B) Distribution of *H. ochrogyna* and *H. striata* population samples from south-eastern Amazonia sequenced in this study. Two samples of *H. ochrogyna* from Rondonia state were also included but are not shown on the map (see Supporting information Table S1 for locality information).**

analyses to determine if the widths of clines for individual loci were narrower than expected under neutral dynamics and whether the variance in cline widths and center indicated that different genomic regions were behaving in a highly concerted fashion. We come to similar general conclusions for *H. striata* and *H. ochrogyna* as for the older pairs of cryptic Amazonian taxa thus far studied, that intrinsic postzygotic isolation is strongly developed, prevents or greatly reduces introgression across most of the genome and is largely responsible for the maintenance of species boundaries.

Methods

POPULATION SAMPLING

We sequenced a total of 166 *Hypocnemis* specimens belonging to *H. ochrogyna* and all currently recognized subspecies of *H. striata* (*H. s. affinis, H. s. implicata, and H. s. striata;* Isler et al. 2007a, see Supporting materials for more details) collected in a north to south transect in the region between Teles Pires and Xingu Rivers. Special emphasis was placed on sampling at two localities (Fazenda Pium/Agua Azul and Fazenda Jarina) where both parental species were encountered in proximity. Collecting expeditions to Fazenda Pium occurred in 2012, 2015, and with a broader sampling effort in 2018, and to Fazenda Jarina in 2015, with detailed sampling in 2018. Voucher specimens were deposited in the Museu Paraense Emílio Goeldi Brazil (MPEG).

DE NOVO GENOME SEQUENCING

We made use of an unpublished draft genome of *H. ochrogyna* from a related lab project and briefly describe its sequencing and assembly here. Pectoral tissue from a male individual (collectors number: JTW 1514; study skin deposited at the Goeldi Museum: specimen number MPEG 79990) from Marcelândia Brazil (-11.112°S, -54.261°W) was sent to Hudson Alpha for high molecular weight DNA extraction and whole-genome sequencing. A Chromium 10× library was prepared and paired-end sequenced (with a median 306bp insert size) along with a different species of suboscine bird on a single HiSeq X Illumina lane by Hudson Alpha. Genomic scaffolds were processed and assembled by us using default settings on the Supernova 1.2.2 (Weisenfeld et al. 2017) pipeline. The pipeline was run using 28 threads (two threads per CPU core) and a maximum of 185 gigabytes of memory on a single server node containing two Xenon E5-2670 central processing units. The resulting scaffolds were aligned to the chromosomes of the *Ficedula albicollis* genome (Genbank Accession: GCA_000247815.2; Ellegren et al. 2012) using Minimap2-2.17 (Li 2018) with the following options: "-ax asm20." Chromosomal identities were retained for scaffolds with MAPQ alignment scores greater than 57 and which aligned to only one *Ficedula* chromosome. While intrachromosomal rearrangements are common in birds, interchromosomal rearrangements are rare (Ellegren 2010). Chromosomal information was used only to identify SNP pairs on different linkage

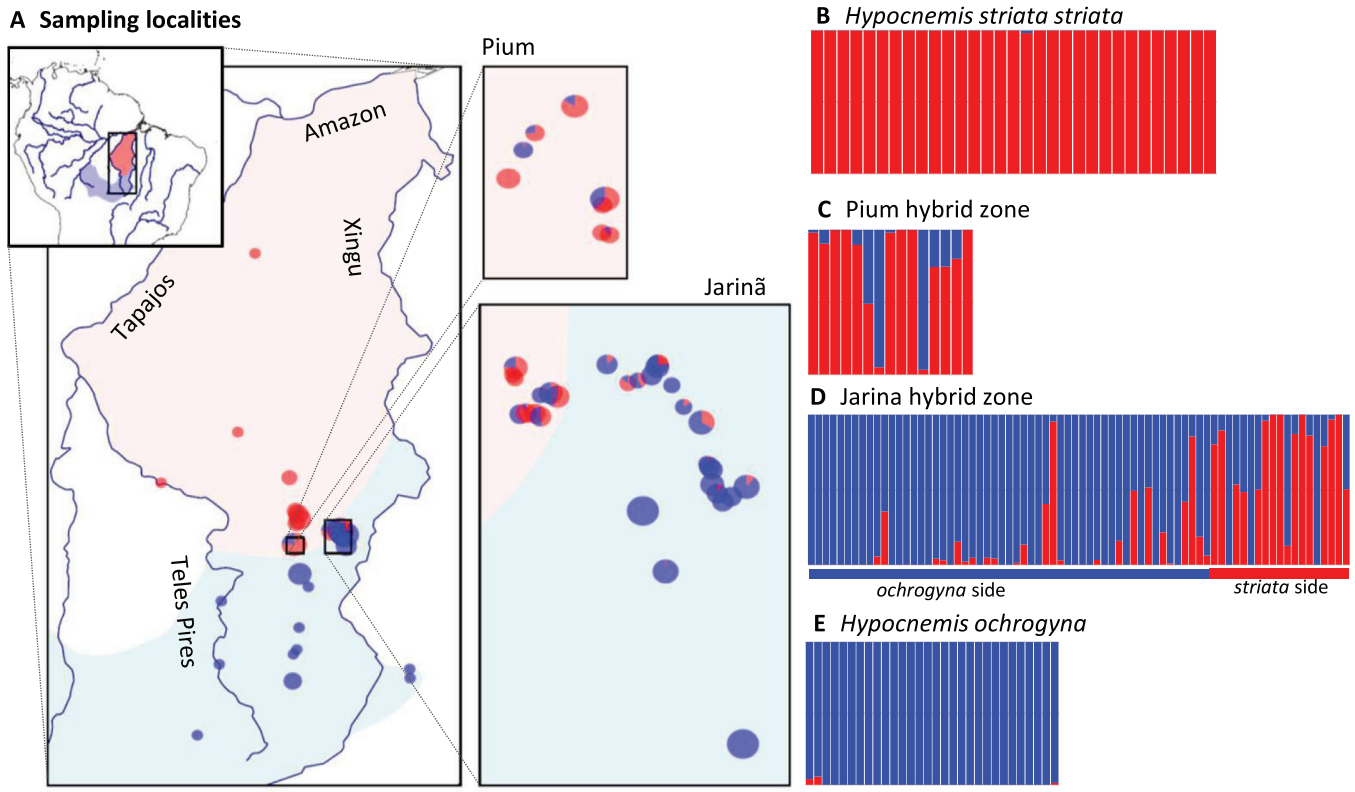

Figure 3. **Analyses of population structure and admixture in 146 individuals of *Hypocnemis ochrogyna* (blue) and *H. striata* (red). The contact zone center between the geographic ranges of *H. ochrogyna* (pale blue) and *H. striata* (pale red) was estimated using kriging of the admixture proportions of individuals. Pie charts in A (with size of pie proportional to the number of individuals from the locality) and bar charts in B to E show admixture proportions. Genetically admixed individuals occur at Fazenda Pium and Fazenda Jarina. Admixture proportions in C and D are ordered based on their distance from the hybrid zone center, with coloured horizontal bars in D showing the *H. ochrogyna* and *H. striata* sides of the contact zone. Two *H. ochrogyna* samples from the state of Rondonia to the west are off the map and not shown.**

groups to estimate interchromosomal linkage disequilibrium (see below).

GENOTYPING-BY-SEQUENCING AND SNP GENERATION

DNA was extracted from muscle tissue using an Omega Biotek E.Z.N.A DNA Extraction Kit. DNA concentrations were assessed with a QuBit® 2.0 Fluorometer (Thermofisher), using a Qubit® hsDNA Assay (Life Technologies). Two Genotyping-by-Sequencing (GBS) libraries were created in-house for 123 individuals of *Hypocnemis* and 71 individuals of other bird species following the protocol of Elshire et al. (2011) with modifications by Alcaide et al. (2014) and is only briefly outlined here. Genomic DNA of each sample was individually barcoded. Genomic DNA for each individual was digested with PstI and individual specific barcodes and common adaptors were ligated onto the resulting fragments. Samples were cleaned with AMPure XP beads (Beckman-Coulter) at a ratio of 23:15, and 18 rounds of PCR amplification were performed prior to pooling, using Phusion-Taq (New England Biolabs) with the following protocol: denaturation at 98°C (30 sec) then 18 cycles of 98°C (10 sec), 65°C (30 sec), and 72°C (30 sec), with a final 72°C extension step (5 min). For each library, 100 ng of DNA for 94 individuals were then pooled and size-selected on a 2% agarose gel to retain fragments between 150 and 300bp and 350 and 1000 bp using a QIAquick Gel Extraction Kit (Qiagen). An extremely bright and sharp peak between 300 to 350 bp was excluded as it likely represented a fragment generated due to cut sites in mitochondrial DNA. The size distribution of library fragments was determined by running 3 μL of the final library on a Bioanalyzer. For each library, paired-end sequencing was performed on a single lane of Illumina HiSeq4000 and an average of 5.7 million (range 3.4 to 17.0) 100 bp reads were obtained per individual. In addition, DNA of 43 individuals of *Hypocnemis* was sent to the Cornell Institute for Genomic Diversity for GBS using similar methods with approximately 2 million 100 bp reads per individual obtained using Illumina HiSeq2000 single-end sequencing.

All 166 individuals were demultiplexed using *process_radtags* from the STACKS 2.3 (Catchen et al. 2011; Catchen et al. 2013) pipeline with the following options: -e pstI -r -c -q -t 90 -w 0.15 -s 10 -i gzfastq –adapter_mm 1. For our two paired-end libraries, paired reads were combined. Reads were further trimmed and filtered based on sequencing quality using Trimmomatic-0.38 (Bolger et al. 2014) with options set as: TRAILING:3 SLIDINGWINDOW:4:10 MINLEN:30. The resulting reads were aligned to the unpublished *H. ochrogyna* reference genome using Bowtie2 with options set as: –very-sensitive -N 1 –score-min L,-0.6,-0.6. Read alignments were filtered to exclude those with alignment scores <10 and in which the best (AS) and second best (XS) alignment scores differed by less than a value of 10 (equivalent to two mismatches at high quality reads) and were outputted as sorted and indexed bam files using the sort and index functions of Samtools 1.3 (Li et al. 2009). SNPs were then called using *ref_map.pl* pipeline of STACKS 2.3 using default options except that we invoked the following string of options, "–unpaired -X gstacks:–max-insert-len 600 -X populations:-t 12 -e pstI –merge_sites –ordered_export." SNPs were exported as a vcf file.

We generated three datasets. Dataset 1 included all 166 individuals from all libraries and was used only for analysis of population structure and admixture. Dataset 2 included only individuals of *H. ochrogyna* and *H. striata striata* (n = 146) from the paired-end libraries which received much greater sequencing depth and was used in all other analyses. Datasets 1 and 2 were filtered in *vcftools* (Danecek et al. 2011) in the following order: (1) genotype calls with less than 5× coverage were treated as missing data; (2) SNPs with missing genotype calls for more than 50% of individuals were excluded; (3) SNPs with average sequencing depth exceeding the 95th percentile were excluded (to exclude potential paralogues incorrectly aligned together as a locus; (4) SNPs with a minor allele frequency less than 5% were excluded; (5) SNPs with observed heterozygosity exceeding 0.75 were excluded (to exclude potential paralogues incorrectly aligned together as a locus); (6) individuals with missing genotype calls at more than 80% of SNPs were excluded; (7) SNPs with less than three copies of the minor allele were filtered out (necessary as steps 5, 6, and 7 may have rendered some SNPs monoallelic following minor allele frequency filtering in step 4); (8) SNPs were thinned to be a minimum of 10,000 bp apart on the reference genome. Dataset 3 was identical to Dataset 2 except that the final thinning step was not performed in order to retain more SNPs for F_{st} analyses where independence of loci is not an assumption of the method.

GENOMIC ANALYSES

Population structure and admixture: Principal coordinate analyses using Euclidean distances (PCoA) were performed in PAST v.3.23 (Hammer et al. 2001) using the entire Dataset 1 (see Supporting information Table S1 for more details). Admixture 1.3.0 (Alexander et al. 2009) was run on *H. ochrogyna* and *H. s. striata* individuals from Dataset 1 to assess population structure, the location of hybrid zones, and admixture proportions of hybrid individuals. Admixture was run for K = 1 to 11 populations using default parameters. The best K was assessed using the built-in cross validation method of Admixture.

Interchromosomal linkage disequilibrium, heterozygosity, and hybrid index: We used 1079 fully fixed SNPs between parental populations outside of the hybrid zone to calculate three statistics: pairwise interchromosomal linkage disequilibrium (*D'*) between all SNP pairs was calculated using the R package LDheatmap (Shin et al. 2006) and hybrid index (analogous to admixture proportions from the program Admixture but calculated using only the fixed SNPs) and observed heterozygosity were calculated using the R package Introgress (Gompert and Buerkle 2010) and following the methods in Pulido-Santacruz et al. (2018). These three measures were used to infer the presence of strong postzygotic isolation and were performed on hybrids from both Pium and Jarina. Calculating *D'* only for SNP pairs from different chromosomes has the advantage of eliminating linkage disequilibrium between SNPs that arises simply due to close physical linkage. Interchromosomal linkage disequilibrium within a hybrid zone can be generated in several ways including: (1) ongoing immigration of parental genotypes into the hybrid population, (2) epistatic interactions between loci on different chromosomes (e.g. genetic incompatibilities are one example), and (3) strong premating selection reducing formation of hybrids or strong postzygotic isolation reducing fitness of hybrids.

Because fully fixed SNPs are used, F_1 hybrids should be heterozygous at all SNPs and, thus, have an observed heterozygosity of 1 and a hybrid index of 0.5. F_2 hybrids retain a hybrid index of close to 0.5 but have an observed heterozygosity of 0.5. First, second, third, and fourth generation backcrosses between an F_1 and a parental species will have observed heterozygosity values close to 0.5, 0.25, 0.125, and 0.0625, respectively, and hybrid indices of 0.25, 0.125, 0.0625, and 0.03125 when crossed into *H. ochrogyna*, and 1.0 minus these values when crossed into *striata*. Importantly, individuals which have backcrossed only into one of the two parent species will lie on the diagonals of the triangle plot while all off-diagonal individuals represent F_2 hybrids, later generation hybrids with an F_2 in their ancestry, or result from a cross between backcrossed individuals from opposite diagonals of the triangle plot. These off-diagonal individuals have the most heavily recombined genomes and may be most susceptible to selection against genetic incompatibilities.

We simulated the expected distribution of triangle plots following methods in Pulido-Santacruz et al. (2018) under a neutral scenario of no selection against hybrids and under

assortative mating (with mating probability tied to similarity in hybrid index), and postzygotic selection against 25 Dobzhansky-Muller incompatibilities (DMI model hereafter) with a selection rate of 0.035 against each DMI. R code to replicate the simulations is provided in the Supporting online materials. We allowed individuals in the hybrid population to be replaced by an immigrant *H. ochrogyna* with a probability of 0.05 or *H. striata* with a probability of 0.05 at each year. Thus, on average a total of 10% of individuals in the hybrid population are replaced by parental immigrants each year. We then repeated these simulations with a moderate (20% replacement) and high (30% replacement) immigration scenarios. Each simulation used 68 individuals (the number of hybrid zone individuals in our empirical dataset from Dataset 2) and the same number of SNPs (1079) as in our empirical dataset from hybrid zone populations, but assumed no physical linkage between markers (e.g. genetic incompatibilities occur between loci on separate linkage groups). We also calculated *D'* for the four simulations of heterozygosity and hybrid index with or without selection against hybrids and under two low and high levels if immigration of parental genotypes. Simulations were run for 1000 generations and a total of 100 simulations were performed to generate triangle plots while density curves of *D*' were plotted for the first 15 simulations to illustrate the range of variation across simulations

Geographic clines: The location of the cline center was estimated as the 0.5 isocline estimated by kriging admixture coefficients (from the Admixture program) across the spatial landscape. The distance of each individual from the cline center was then obtained with the *H. striata* side of the zone indicated as positive distances, and *H. ochrogyna* as negative ones. Geographic clines were fit only for the Jarina hybrid zone where individuals were sampled on both sides of the cline center. Pium samples were excluded because we sampled hybrids only on the *H. s. striata* (e.g. north) side of the hybrid zone center (Fig. 3A). A geographic cline of the genome-wide admixture proportion was generated in the R package HZAR (Derryberry et al. 2014) using a sigmoidal model. Admixture proportions of *H. ochrogyna* and *H. striata* were set at 1 and 0, respectively. The model estimated the cline center, *c*, width, *w*, and their 95% confidence intervals. We then calculated F_{st} in VCFtools between all parental populations located outside of the Pium and Jarina hybrid zones. Only loci with a minimum F_{st} of 0.5 were retained for geographic cline analyses of individual SNPs. We then fit a clinal model with two additional parameters representing the allele frequency in parental populations of each species: allele frequencies in *H. ochrogyna* and *H. striata* are designated as $P_{ochrogyna}$ and $P_{striata}$, respectively. ΔP is $P_{ochrogyna}$ minus $P_{striata}$ while the width is ΔP divided by the slope at *c*. Clines were fit using HZAR and only clines with a ΔP of 0.5 or greater were retained. Individual loci were considered outliers if the 95% confidence intervals of their *w* and *c* parameters did not overlap the 95% confidence intervals from the genome-wide admixture cline

Assessment of gene flow into parental populations: We used Hudson's F_{st} (Hudson et al. 1992) to assess whether genes are introgressing through the hybrid zone into adjacent heterospecific parental populations. To this end, we split parental populations into two groups. Those which are between 50 and 100 km from the hybrid zone center (given the narrow hybrid zone widths, these are well outside of the hybrid zone region) and those which are greater than 100 km. Hudson's F_{st} was compared between the distant and close populations using Dataset 3. If our hybrid zone is behaving in a largely neutral fashion (e.g. with few SNPs closely linked to genetic incompatibilities or other loci under selection not to introgress) then we expect loci to have introgressed into nearby parental populations resulting in greatly reduced F_{st} for most SNPs. In contrast, we expect that with sufficient numbers of genetic incompatibilities, our genomes will become nearly impervious to introgression even at neutral sites and F_{st} will not be reduced in near versus far parental populations. An intermediate scenario, where only a subset of loci has reduced F_{st} would indicate a hybrid zone that is acting as a semipermeable membrane, allowing some loci to introgress but not others. Two analyses were performed. The first included 48,709 SNPs from Dataset 3 which had at least five individuals for each of the four parental populations. A genome-wide value of Hudson's F_{st} was calculated and 1000 nonparametric bootstrap replicates were used to generate 95% confidence intervals. The second used the same 48,709 SNPs as in the first analysis but calculated Hudson's F_{st} across individual genomic scaffolds (excluding scaffolds with fewer than 10 SNPs) and compared scaffold F_{st} between close versus far populations using a paired *t*-test for either all SNPs or for SNPs with interspecific $F_{st} > 0.5$ for the combined far and close populations.

Results

DE NOVO GENOME SEQUENCING

We obtained 226 million reads. Mean read lengths after trimming (Supernova automatically trims the first 23 bases that includes a 10× barcode and 7 additional bases) was 140 bp. Reads were assembled into molecules with weighted average length of 40 kb and these were assembled into a draft genome comprising 81,824 scaffolds ranging in size from 1 kb to 3.3 Mb with a contig N50 of 62.1 kb and a scaffold N50 of 451.54 kb. Total genome size of scaffolds exceeding 1 kb (those under 1 kb were excluded) was 1.05 Gb suggesting our assembly contains most of the anticipated 1.1 to 1.2 Gb genome typical of passerine birds. Effective median coverage (following base trimming) as estimated by Supernova 1.2.2 was 47.8×.

DE NOVO GENOME SEQUENCING

Following filtering, Dataset 1 contained 20,440 SNPs for 152 individuals. Dataset 2 contained 26,460 SNPs for 108 individuals. Dataset 3 contained 93,309 SNPs for 108 individuals. Admixed individuals were detected at two general sampling locations: Fazenda Pium (−10.5°S, −54.4°W) and Fazenda Jarina (−10.3°S, −53.6°W) (Figs. 2, 3) which are located 90km apart.

GENOMIC ANALYSES

Population structure and admixture: Principle coordinate analyses using Dataset 1 uncovered three distinct clusters: (1) *H. ochrogyna*, (2) *H. striata striata*, and (3) *H. s. affinis* and *H.s. implicata* combined (Fig. 2). The last cluster included two subspecies whose geographic distributions are fully isolated by the intervening *H. s. striata*. Individuals from Fazenda Pium and Fazenda Jarina formed a clinal gradation along principal coordinate 1 and represent a hybrid zone between the first two groups.

The best-fit number of genetically distinct populations (using only localities within the range of *H. ochrogyna* and *H. s. striata*) obtained by Admixture's cross-validation test was two (Fig. 3). Sixty-seven individuals were collected from localities with at least 1 admixed individual at Fazenda Jarina (Fig. 3D). These included 11 individuals with minor (2 to 4.9%), 13 with moderate (5 to 24.9%), and 10 with extensive (25 to 50%) admixture. We also found 28 *ochrogyna*-like individuals (26 that were >99.9% *H. ochrogyna*) and five individuals similar to *H. s. striata* (four that were >99.9% *H. s. striata*). In addition, the furthest site south on the Jarina map inset in Figure 3A included *H. ochrogyna* individuals with no apparent admixture with *H. striata striata*. Fourteen individuals were sampled from Pium (Fig. 3C) including two individuals with minor (2 to 4.9%), three with moderate (5 to 24.9%), and three with extensive admixture (25 to 50%) as well as six individuals that were *H. s. striata*-like (five >99.9% pure *H. s. striata*). No individuals represented pure *H. ochrogyna* though two *H. ochrogyna*-like individuals contained only low levels of introgression from *H. s. striata*. Kriging of admixture proportions (Fig. 2) placed the hybrid zone center to the south of our Pium sampling sites but running through our sampling transect at Jarina. Individuals that were almost pure *H. striata striata* and *H. ochrogyna* were collected within 100 m of each other indicating a hybrid zone narrow enough that parentals of both species meet and have the opportunity to produce F_1 hybrids. In Jarina, three individuals with genomes >99.9% *H. ochrogyna* occurred on the *H. striata* side of the hybrid zone, the furthest of which was located 3.0 km from the cline center and was located just 60 m from an individual whose genome was 86% *H. striata*. One individual with 95% *H. striata* genome was located 11.6 km from the cline center on the *H. ochrogyna* side and was collected 350 m away from a pure *H. ochrogyna* individual.

IInterchromosomal linkage disequilibrium and heterozygosity, hybrid index: A histogram of linkage disequilibrium and triangle plot of observed heterozygosity and hybrid index of individuals from the Pium and Jarina populations of the hybrid zone are shown in Figure 4A and 4B, respectively. The hybrid index uses only SNPs fixed between parental populations outside of the hybrid index but was strongly correlated with hybrid index calculated with Admixture using all SNPs (Pearson's $r = 0.998$). D' for 68 hybrid zone individuals at 1079 diagnostic SNPs ranged from 0.17 to 1.0 in the contact zone with a median D' of 0.84 (Fig. 4A). Five individuals represent F_1s and one individual occurred in the off-diagonal middle region of the triangle plot and represents an individual with a heavily recombined genome. All remaining individuals either possessed parental-like genomes or represent backcrosses along the diagonals of the triangle plot.

Simulations of linkage disequilibrium, observed heterozygosity, and hybrid index are illustrated in Figure 4C-G. Stable dynamics were generally reached after just 4 to 10 generations with patterns changing little at 10, 100, and 1000 generations (Fig. 4C). These indicate that under neutral dynamics many admixed individuals are expected to occur in the off-diagonal regions of the triangle plot and to have low levels of interchromosomal linkage disequilibrium ranging from a median value of $D' \leq 0.4$ under the low immigration scenario to no higher than 0.6 under the high immigration scenario. Adding a high value of premating isolation (assortative mating value of 0.7 indicating females reject prospective heterospecific mates 70% of the time) had only a minor effect on these distributions. When premating isolation was set to be very high (0.9) under a high immigration scenario, hybrid index became more bivariate, but even under these conditions many individuals are expected to occur in off-diagonal regions of the triangle plot. In contrast, the simulations with intrinsic postzygotic isolation generated few individuals in the off-diagonal regions (e.g. hybrid index is strongly bimodal, but with a slight excess of F_1 hybrids) and have high (median $D' = 0.8$) to very high (median $D' = 0.95$) levels of interchromosomal linkage disequilibrium under the moderate and high immigration simulations, respectively.

Geographic clines: The genome-wide cline of admixture proportions had a center at −1.61 km (95% CI: -3.45 to 0.94 km) indicating a close correspondence to the estimate of the cline center based on kriging of admixture values. Genome-wide cline width was 15.4 km (95% CI: 11.9 to 19.7 km). For 5302 loci with $\Delta P \geq 0.5$, 1 had a significantly narrower and 70 had significantly broader cline width than the genome-wide cline and 33 and 30 loci had cline centers shifted significantly toward the *H. ochrogyna* or *H. striata striata* sides of the cline center, respectively. The central 95% (i.e. values between 2.5 to 97.5 percentiles) of cline widths occurred between values of 4.2 and 57.5 km and cline centers between −9.7 and

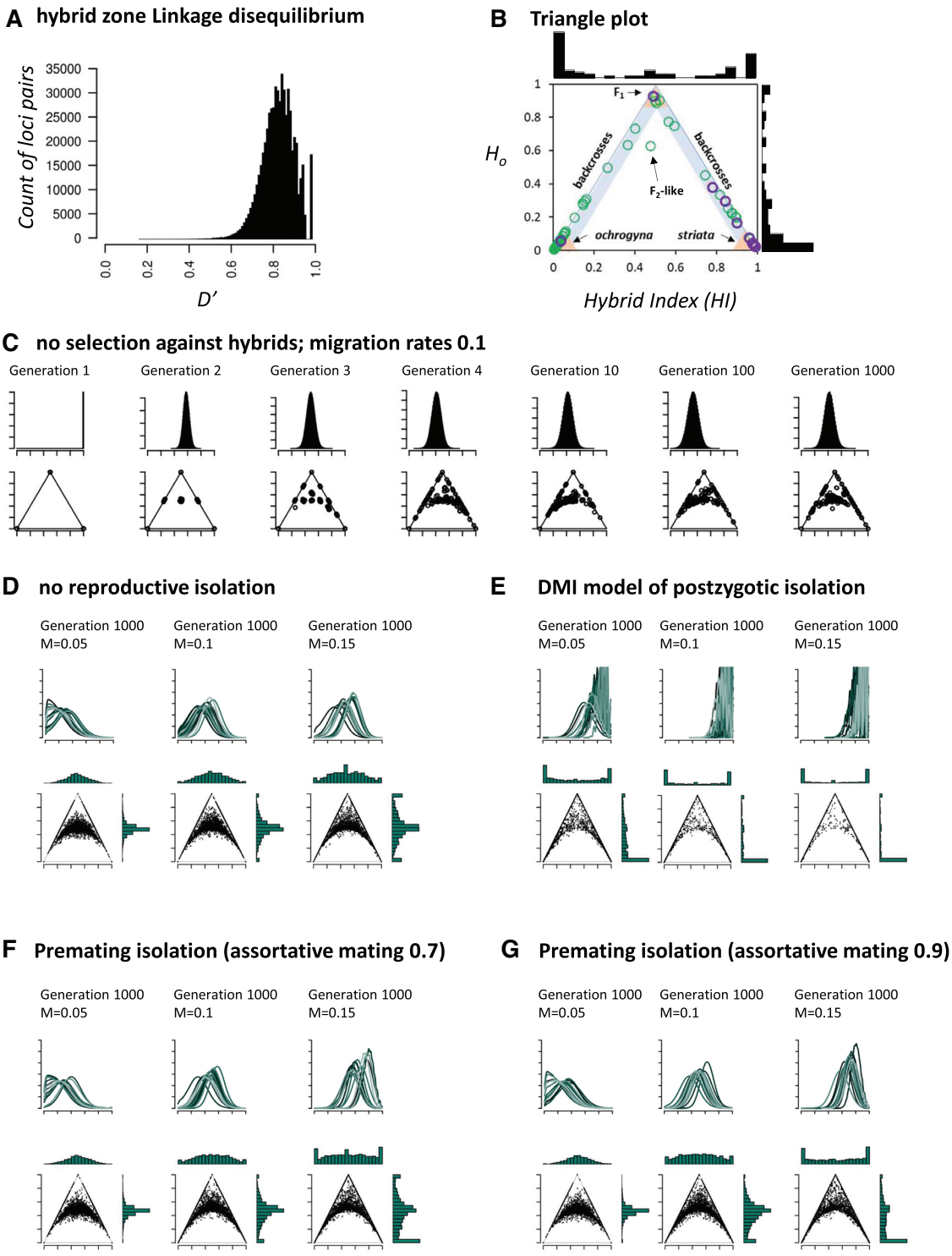

Figure 4. Analyses of linkage disequilibrium (*D*′), observed heterozygosity (*Ho*), and hybrid index (*HI*). (A) Shows interchromosomal *D*′ for 1079 SNPs fixed in parental populations for 68 individuals from hybrid zone populations. (B) Shows a triangle plot of hybrid index and observed heterozygosity calculated for the same dataset for hybrid zone populations at Pium (purple) and Jarina (green). (C to G) Illustrate example simulations of *D*′ (top row) and observed heterozygosity and hybrid index (bottom row) for varying levels of immigration of parental into hybrid zone populations and of assortative mating or postzygotic selection against hybrids. Panel C follows a single simulation of 68 individuals for 1000 generations. Plots of *D*′ in D to F show density curves (*y*-axis tick marks represent a density increase of 1.0) for 15 different simulations. Triangle plots in D to F are based on 100 simulated datasets, each with 68 individuals (prior to selection steps at each generation) and 1079 SNPs. An assortative mating value of 0.7 indicates a female will reject 70% of prospective heterospecific mates.

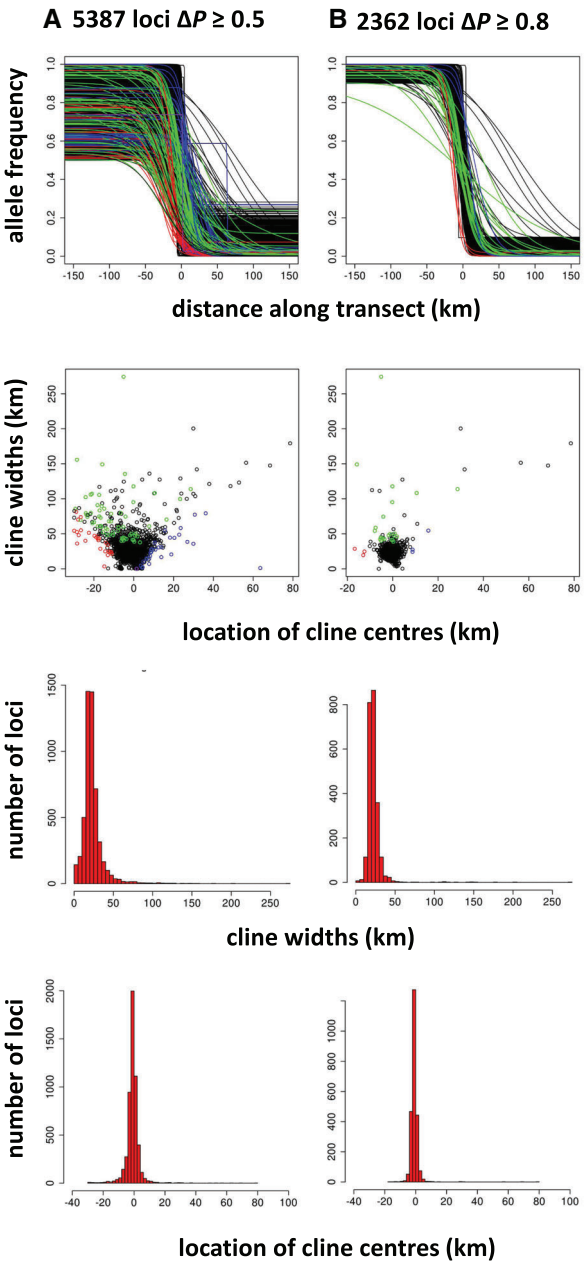

Figure 5. Analyses of geographic clines for SNPs with (A) ΔP greater than 0.5 and (B) ΔP greater than 0.8 (see text for details). Loci with widths greater (green) or narrower (pink) than expected or with cline centers significantly shifted toward *H. ochrogyna* (red) or *H. striata* (blue) are shown.

6.3 km. For 2362 highly differentiated loci (Fig. 5) with $\Delta P \geq 0.8$ (and with $P_{ochrogyna}$ greater than 0.9 and $P_{striata}$ less than 0.1), none had narrower and 22 had broader cline widths than the genome-wide cline and 3 loci had cline centers shifted significantly toward *H. ochrogyna* and 3 toward *H. striata striata*. The central 95% of cline widths occurred between values of 13.4 and 37.8 km and cline centers between −4.2 and 2.7 km.

Assessment of gene flow into parental populations: Interspecific Hudson's F_{st} calculated from across the genome was nearly identical and overlapped in 95% confidence intervals for close (F_{st}= 0.552, 95% CI 0.548-0.556) versus far (F_{st} = 0.553, 95% CI 0.549-0.557) parental populations. Likewise, Hudson's F_{st} calculated for each genome scaffold were very similar between close and far populations and paired *t*-tests were nonsignificant when either all scaffolds with 10 or more SNPs were used (n = 1074, mean of difference between far versus close = −0.00084, $t = -0.384$, $p = 0.70$) or when only highly differentiated scaffolds with an interspecific Hudson's F_{st} exceeding 0.5 were used (n = 633, mean of difference between far versus close = 0.00089, $t = 0.345$, $p = 0.73$).

Discussion

Here, we investigate levels of reproductive isolation along a contact zone between two highly cryptic lineages of *Hypocnemis* antbird. We found multiple lines of evidence that despite being highly cryptic and despite extensive hybridization at the contact zone as revealed by many individuals exhibiting a range of admixture values, speciation is essentially complete with high levels of postzygotic isolation resulting in only a very small amount of the genome introgressing across species barriers.

Our first line of evidence for reproductive isolation comes from comparing levels of interchromosomal linkage disequilibrium (*D'*) within our hybrid zone populations to linkage disequilibrium values from simulations with or without reproductive isolation and under low to high levels of gene flow from parental populations. Because we compared *D'* across SNPs which are fixed between parental populations outside of contact zones, a lack of F_2 and later generation hybrids (including backcrosses with parental populations), would result in a *D'* value of 1.0 for each SNP pair within the hybrid zone. Our empirical values (Fig. 4A) are less than 1.0 for all but a small proportion of SNP pairs indicating that admixture has led to some breakdown of linkage disequilibrium. However, in the absence of any reproductive isolation, our simulations indicate that geneflow from parental populations can only maintain low to moderate levels of *D'* through time (Fig. 4C, D). Increasing migration rate resulted in higher *D'*. Our high immigration scenario results in approximately 30% of individuals in each year representing immigrants from outside parental populations. While we have not measured immigration rates directly, low dispersal capabilities typically associated with Amazonian understory-dwelling forest birds, such as *Hypocnemis* (Develey and Stouffer 2001; Woltmann et al. 2012), render it highly unlikely that 30% or more of contact zone individuals are replaced by parental immigrants each year. Rather, our empirical distribution of *D'* had a larger mode than even the high dispersal simulations suggesting that

immigration alone cannot account for the empirical pattern (compare Fig. 4A and D). In contrast, adding premating isolation had a modest effect and postmating isolation a major effect on maintaining an elevated distribution of *D'*.

Triangle plots of observed heterozygosity and hybrid index in hybrid populations provide strong evidence for selection against hybrids. Our empirical results closely match those simulated with Batesian—Dobzhansky–Muller incompatibilities under low to moderate levels of immigration (Fig. 4E). The empirical triangle plot revealed six F_1-like hybrids as well as a series of individuals representing successive generations of backcrossing into each parental species (Fig. 4B). Surprisingly, we only encountered one individual consistent with an F_2-like hybrid and found no additional individuals that occur in the off-diagonal positions of the triangle plot where a large proportion of individuals in a hybrid zone should occur if there is no selection against hybrids (Fig. 4D,F,G). Importantly, hybrids in off-diagonal positions possess highly recombined genomes and their near absence in the hybrid zone is a strong indicator that genetic incompatibilities, often most deleterious in a heavily recombined state (e.g. the "pathway" model of epistatic incompatibilities sensu Lindtke and Buerkle 2015; or recessive Batesian—Dobzhansky–Muller incompatibilities), generally render individuals with highly recombined genotypes inviable. Our empirical results closely match those simulated with Batesian—Dobzhansky–Muller incompatibilities under low to moderate levels of immigration.

Previous analyses under moderate levels of immigration have demonstrated that even very high levels of assortative mating (up to 99%) are incapable of preventing the formation of numerous off-diagonal hybrids (Pulido-Santacruz et al. 2018), thus, their near absence is an indicator for selection against heavily recombined genotypes rather than strong premating barriers. Our triangle plot simulations here confirm this result under a broader range of immigration rates. While high immigration and strong assortative mating (Fig. 3G) are capable of generating a bivariate distribution of hybrid indices, they continue to exhibit an excess of off-diagonal hybrids (as evidenced by the excess of simulated individuals with H_o near 0.5) that fail to match our empirical data. However, high levels of immigration would also lead to emigration of hybrids into adjacent parental populations, likely accelerating hybrid zone expansion rather than narrowing it, an effect we did not consider in our model but which has been modeled and confirmed elsewhere (Irwin 2020). These results, together with the fact that we have a hybrid zone where hybridization is common, argues against strong premating isolation for our species pair but does not eliminate a secondary contribution of assortative mating to total reproductive isolation.

The presence of substantial numbers of backcrossed individuals along the diagonals of the triangle plot might indicate that introgression into a heterospecific background is still possible despite selection against heavily recombined genotypes. How much of the genome is capable of introgressing through successive generations of backcrossing should largely depend on the proportion of the genome that is not closely linked to genetic incompatibilities. During early stages of genomic divergence, few incompatibilities allow most of the genome to introgress. During late stages of the speciation process, large numbers of incompatibilities render most of the genome immune to introgression. We calculated geographic cline width of individual loci to determine the number of loci for which bidirectional introgression is eroding away species differences. Expected cline widths under neutral dynamics are governed by postnatal dispersal distance (larger distances result in broader clines) and the number of generations since secondary contact. Postnatal dispersal distances have been estimated for only one avian Neotropical species, *Myrmeciza exsul*, which disperses on average only 1.1 km (Woltmann et al. 2012). This species belongs to the same family as *Hypocnemis*. Assuming *Hypocnemis* disperses similar distances, has a generation time of two years, and that secondary contact for *Hypocnemis* and the other six known hybrid zones in the headwaters between the Teles Pires and Xingu rivers formed approximately 11,500 years ago following postglacial expansion of forest along the southern edge of Amazonia (see Weir et al. 2015), hybrid zone widths should be about 211 km on average. Only 1 of 5387 loci had a cline width exceeding this expectation (Fig. 5), while 95% of loci had cline widths less than 45 km and the median cline width was only 21 km. These results suggest selection acting against introgression is strong and that very few loci are able to introgress as deeply as a reasonable neutral expectation.

Cline centers for individual loci are also expected to show considerable variability due to neutral processes when they are not closely linked to genetic incompatibilities, while selection for a locus to introgress into a heterospecific background may cause its cline center to be greatly displaced relative to other loci. However, we found very little variability in cline center (Fig. 5). This tight coupling of cline centers and very narrow cline widths are further reflected in nearly identical interspecific Hudson's F_{st} values between parental populations located far (greater than 100 km away) versus near the contact zone center (50 to 100 km away) and suggest that very few loci are capable of introgressing even short geographic distances into a heterospecific background. Together these results suggest that these two species have left the intermediate stage of the speciation process where neutral parts of the genome remain semipermeable to geneflow in regions not closely linked to genetic incompatibilities and instead argue strongly for a late stage in the speciation process, where, despite what appears to be a lack of strong levels of premating isolation, sufficient numbers of genetic incompatibilities

spread across the genome have rendered most of the genome immune to introgression.

Hypocnemis ochrogyna and *H. striata* together with five other currently recognized species that make up the *Hypocnemic cantator* complex were long considered conspecific given their high degree of similarity in plumage and territorial song (see Fig. 1). Their current treatment as full species rests largely on the presence of diagnostic differences in song and call (Isler et al. 2007a) which, though detectable on sonograms (e.g. Fig. 1), are nevertheless remarkably similar. However, playback experiments of songs between several allopatric taxa pairs in this complex continue to illicit strong aggressive responses suggesting that song differences may often not be recognized by the birds themselves (Weir and Price 2019), though premating isolation generated by call differences between allopatric taxa has not been tested. The presence of a hybrid zone between *H. ochrogyna* and *H. striata*—whose pace differences (evident in Fig. 1) in male song render them one of the most vocally divergent pairs of taxa within the complex (Isler et al. 2007a)—demonstrates this level of vocal differentiation is insufficient to drive strong levels of premating isolation, though some premating isolation likely results. Rather, our evidence for strong levels of intrinsic postzygotic isolation support full species status for this pair and probably more generally for taxon pairs of similar age within the *H. cantator* complex. We are not discrediting a contribution of vocal difference to reproductive isolation, simply that it is unlikely that vocal differences are sufficient on their own to prevent species collapse upon secondary contact without postmating isolation (see also Irwin 2020).

Our results have important implications for our understanding of species richness in Amazonian birds because they suggest that taxon pairs which are morphologically cryptic, weakly differentiated behaviorally, and which appear to have evolved incomplete species discrimination are nevertheless speciating primarily through the evolution of intrinsic postzygotic isolation, with premating isolation playing a more minor role due to its slower accumulation. While a past study on Amazonian hybrid zones in a cryptic pair of antbirds and woodcreepers suggested the same (Pulido-Santacruz et al. 2018), the two pairs in that earlier study were older (i.e. 2.5 to 4.1 mya), and the buildup of high levels of intrinsic postzygotic isolation might be expected for such old taxon pairs. Here, our results for *H. ochrogyna* and *H. striata*—estimated to have diverged between one and two million years ago (Weir et al. 2015; Silva et al. 2019)—suggest that speciation, driven primarily by strong levels of intrinsic postzygotic isolation, is possible in younger pairs of cryptic Amazonian taxa. Whether this will generally be true depends on whether the buildup of high levels of intrinsic postzygotic isolation in *H. ochrogyna* and *H. striata* was at a pace typical for Amazonia. Genetic incompatibilities are expected to accumulate through time as a byproduct of neutral genome differentiation between all pairs of allopatric taxa. While divergent selection can speed up this process, we have no reason to expect that *H. ochrogyna* and *H. striata* experienced higher levels of divergent selection than other Amazonian taxa. Divergent selection driven by climatic niche, for example, is estimated to be low in birds near the equator in general (Lawson and Weir 2014). If our results for *H. ochrogyna* and *H. striata* hold true for other hybridizing taxa pairs of similar age, then it is likely that the plethora of cryptic Amazonian taxa that continue to be detected by detailed phylogeographic studies will also possess intrinsic reproductive isolation and their recognition as full species would substantially increase species richness in what is already recognized as the most species-rich region on the planet. Our results thus suggest the strong possibility that species richness could be dramatically underestimated in Amazonia, especially for antbirds and other understory specialists.

AUTHOR CONTRIBUTIONS

J.T.W designed the study. A.A.C., A.A., and J.T.W. collected field samples. A.A.C. and E.M. generated GBS libraries, A.A.C. perform analysis of population structure and admixture, and J.T.W. performed hybrid zone simulations and cline analysis. J.T.W and A.C.C. wrote and all authors edited the manuscript.

ACKNOWLEDGMENTS

We gratefully acknowledge the many landowners in Brazil who allowed sampling on their property, in particular the owners and/or managers of Fazenda Juruna and Fazenda Jarina where our greatest field effort was concentrated. The Brazilian National Research Council (CNPq) granted field research permits (4253-1, 40173-1, and 6581-1). Research was funded by the following grants: PDSE-CAPES #88881.189565/2018-01 (A.A.C); CNPq ('INCT em Biodiversidade Uso da Terra da Amazonia' #574008/2008-0; #471342/2011–4; #310880/2012-2; and #306843/2016-1) and the Amazonia Paraense Foundation—FAPESPA (grant no. ICAAF 023/2011) (A.A.); Natural Sciences and Engineering Research Council of Canada (NSERC) CGS-D fellowship (411293437) (E.M.); NSERC Discovery Grants (402013-2011, RGPIN-2016-0653) and an NSERC Accelerator Grant (no. 492890) (J.T.W). We thank Maya Faccio, Paola Pulido-Santacruz, Alfredo Barrera-Guzmán and Sidnei Dantas for assistance with field sample collection; Alfredo Barrera-Guzmán and Carlynne Simões for assistance with DNA isolation and quantification; and Jordan Bemmels for discussions about F_{st}.

CONFLICT OF INTEREST

The authors declare no conflict of interest.

DATA ARCHIVING

Illumina short read data have been deposited in the National Center for Biotechnology Information Sequence Read Archive under BioProject PRJNA665047.

LITERATURE CITED

Alcaide, M., E.S.C. Scordato, T.D. Price, and D.E. Irwin. 2014. Genomic divergence in a ring species complex. Nature 511:83–85.

Alexander, D.H., J. Novembre, and K. Lange. 2009. Fast model-based estimation of ancestry in unrelated individuals. Genome. Res. 19:1655–1664.

Bolger, A.M., M. Lohse, and B. Usadel. 2014. Trimmomatic: a flexible trimmer for Illumina sequence data. Bioinformatics 30:2114–2120.

Catchen, J., P.A. Hohenlohe, S. Bassham, A. Amores, and W.A. Cresko. 2013. Stacks: an analysis tool set for population genomics. Mol. Ecol. 22:3124–3140.

Catchen, J.M., A. Amores, P. Hohenlohe, W. Cresko, and J.H. Postlethwait. 2011. Stacks: building and genotyping loci de novo from short-read sequences. Genes. Genomes Genetics 1:171–182.

Danecek, P., A. Auton, G. Abecasis, C.A. Albers, E. Banks, M.A. DePristo, R.E. Handsaker, G. Lunter, G.T. Marth, S.T. Sherry, et al. 2011. The variant call format and VCFtools. Bioinformatics 27:2156–2158.

Develey, P.E., and P.C. Stouffer. 2001. Effects of roads on movements by understory birds in mixed-species flocks in central Amazonian Brazil. Conserv. Biol. 15:1416–1422.

delHoyo, J., and N.J. Collar. 2016. HBW and Bird Life international illustrated checklist of the birds of the world volume 2: Passerines. Barcelona. J. Field Ornithol. 88;421–424.

Derryberry, E.P., G.E. Derryberry, J.M. Maley, and R.T. Brumfield. 2014. Hzar: hybrid zone analysis using an R software package. Mol. Ecol. Resour. 14:652–663.

Ellegren, H. 2010. Evolutionary stasis: the stable chromosomes of birds. Trends Ecol. Evol 25:283–291.

Ellegren, H., L. Smeds, R. Burri, P.I. Olason, N. Backström, T. Kawakami, A. Künstner, H. Mäkinen, K. Nadachowska-Brzyska, A. Qvarnström, et al. 2012. The genomic landscape of species divergence in Ficedula flycatchers. Nature 491:756–760.

Elshire, R.J., J.C. Glaubitz, Q. Sun, J.A. Poland, K. Kawamoto, E.S. Buckler, and S.E. Mitchell. 2011. A robust, simple genotyping-by-sequencing (GBS) approach for high diversity species. PLoS One 6:1–10.

Fernandes, A.M., M. Wink, C.H. Sardelli, and A. Aleixo. 2014. Multiple speciation across the Andes and throughout Amazonia: the case of the spot-backed antbird species complex (*Hylophylax naevius*/*Hylophylax naevioides*). J. Biogeogr. 41:1094–1104.

Gompert, Z., and A.C. Buerkle. 2010. introgress: a software package for mapping components of isolation in hybrids. Mol. Ecol. Resour. 10:378–384.

Hammer, Ø., D.A.T. Harper, and P.D. Ryan. 2001. Past: paleontological statistics software package for education and data analysis. Palaeontol. Electron. 4:1–9.

Hudson, R.R., M. Slatkin, and W.P. Maddison. 1992. Estimation of levels of gene flow from DNA sequence data. Genetics 132:583–589.

Irwin, D.E.. 2020. Assortative mating in hybrid zones is remarkably ineffective in promoting speciation. Am Natural. 195:E150-E167.

Isler, M.L., P.R. Isler, and B.M. Whitney. 2007a. Species limits in antbirds (Thamnophilidae): the warbling antbird (*Hypocnemis cantator*) complex. Auk 124:11–28.

Isler, M.L., P.R. Isler, B.M. Whitney, and K.J. Zimmer. 2007b. Species limits in the "*Schistocichla*" complex of *Percnostola* Antbirds (Passeriformes: Thamnophilidae). Wilson J. Ornithol. 119:53–70.

Isler, M.L., and B.M. Whitney. 2011. Species limits in antbirds (Thamnophilidae): The scale-backed antbird (*Willisornis poecilinotus*) complex. Wilson J. Ornithol 123:1–14.

Li, H. 2018. Minimap2: pairwise alignment for nucleotide sequences. Bioinformatics 34:3094–3100.

Li, H., B. Handsaker, A. Wysoker, T. Fennell, J. Ruan, N. Homer, G. Marth, G. Abecasis, and R. Durbin. 2009. The sequence alignment/map format and SAM tools. Bioinformatics 25:2078–2079.

Lawson, A.M., and J.T. Weir. 2014. Latitudinal gradients in climatic-niche evolution accelerate trait evolution at high latitudes. Ecol. Lett. 17:1–10.

Lindtke, D., and C.A. Buerkle. 2015. The genetic architecture of hybrid incompatibilities and their effect on barriers to introgression in secondary contact. Evolution (N. Y.) 69:1987–2004.

Orr, H.A. 1995. The population genetics of speciation: the evolution of hybrid incompatibilities. Genetics 139:1805–1813.

Orr, H.A., and M. Turelli. 2001. The evolution of postzygotic isolation: accumulating Dobzhansky–Muller incompatibilities. Evolution (N. Y) 55:1085–1094.

Payseur, B.A. 2010. Using differential introgression in hybrid zones to identify genomic regions involved in speciation. Mol. Ecol. Resour. 10:806–820.

Pulido-Santacruz, P., A. Aleixo, and J.T. Weir. 2018. Morphologically cryptic Amazonian bird species pairs exhibit strong postzygotic reproductive isolation. Proc. R. Soc. B Biol. Sci. 285: 20172081.

Shin, J.-H., S. Blay, J. Graham, and B. McNeney. 2006. LDheatmap: an R function for graphical display of pairwise linkage disequilibria between single nucleotide Polymorphisms. J. Stat. Softw. 16. https//doi.org/10.18637/jss.v016.c03

Silva, S.M., A.T. Peterson, L. Carneiro, T.C.T. Burlamaqui, C.C. Ribas, T. Sousa-Neves, L.S. Miranda, A.M. Fernandes, F.M. D'Horta, L.E. Araújo-Silva, et al. 2019. A dynamic continental moisture gradient drove Amazonian bird diversification. Sci. Adv. 5:1–10.

Whitney, B.M., M.L. Isler, G.A. Bravo, N. Aristizaba, F. Schunck, L.F. Silveira, V.D.Q. Piacentini, M. Cohn-haft, and M.A. Rego. 2013. A new species of antbird in the *Hypocnemis cantator* complex from the Aripuana-Machado interfluvium in central Amazonian Brazil. Pp 282–285. In: J. del Hoyo, A. Elliott, and D. Christie, eds. Handbook of Birds of the World, Vol. 8. Lynx Edicions, Barcelona.

Weir, J.T., M.S. Faccio, P. Pulido-Santacruz, A.O. Barrera-Guzmán, and A. Aleixo. 2015. Hybridization in headwater regions, and the role of rivers as drivers of speciation in Amazonian birds. Evolution (N. Y.) 69:1823–1834.

Weir, J.T., and T.D. Price. 2019. Song playbacks demonstrate slower evolution of song discrimination in birds from Amazonia than from temperate North America. PLoS Biol. 17:1–19.

Weir, J.T., and D. Wheatcroft. 2011. A latitudinal gradient in rates of evolution of avian syllable diversity and song length. Proc. R. Soc. B Biol. Sci. 278:1713–1720.

Weir, J.T., D.J. Wheatcroft, and T.D. Price. 2012. The role of ecological constraint in driving the evolution of avian song frequency across a latitudinal gradient. Evolution (N. Y.) 66:2773–2783.

Weisenfeld, N.I., V. Kumar, P. Shah, D.M. Church, and D.B. Jaffe. 2017. Direct determination of diploid genome sequences. Genome Res. 27:757–767.

Woltmann, S., T.W. Sherry, and B.R. Kreiser. 2012. A genetic approach to estimating natal dispersal distances and self-recruitment in resident rainforest birds. J. Avian Biol. 43:33–42.

Associate Editor: E. P. Derryberry
Handling Editor: T. Chapman

Supporting Information

Additional supporting information may be found online in the Supporting Information section at the end of the article.

Table S1. List of Hypocnemis specimens used in the present study, corresponding to the distribution of the samples represented in Figure 1(c). The acronym MPEG represents the Museu Paraense Emílio Goeldi institution where the samples are deposited.